

## PAPER

 View Article Online  
 View Journal | View Issue

 Cite this: *Green Chem.*, 2023, **25**, 8625

 Received 12th July 2023,  
 Accepted 14th September 2023

DOI: 10.1039/d3gc02517a

rsc.li/greenchem

# Co(dppbsa)-catalyzed reductive *N,N*-dimethylation of nitroaromatics with CO<sub>2</sub> and hydrosilane†

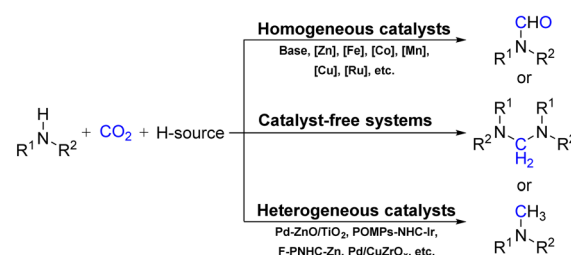
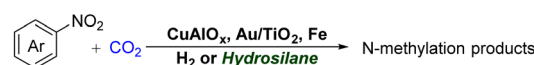
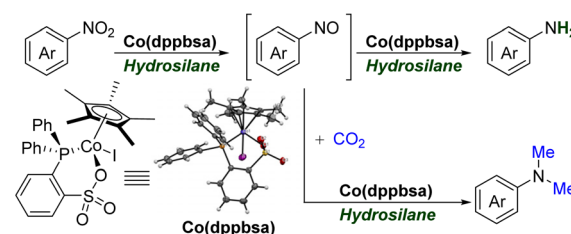
 Shuang-Shuang Ma,<sup>‡a,b</sup> Rui Sun,<sup>‡a,b</sup> Zi-Heng Zhang,<sup>‡c,d</sup> Peng-Xin Guan,<sup>a,b</sup>  
 Jin-Qing Lin,<sup>‡d</sup> Chun-Shan Li<sup>\*a,b</sup> and Bao-Hua Xu<sup>‡a,c</sup>

In this study, a novel half-sandwich phosphinesulfonate cobaltic complex (Co(dppbsa)) was prepared and characterized, which surprisingly enabled the chemoselective *N,N*-dimethylation of nitroaromatics with CO<sub>2</sub> using NaBAR<sub>4</sub><sup>F</sup> as the promotor and a combination of PhSiH<sub>3</sub> and Et<sub>3</sub>SiH as the reductant. Further studies demonstrated that the catalytic activity for reduction of nitroaromatics and CO<sub>2</sub> could be modulated, respectively, by using a specific structure and composition of hydrosilanes. The semi-reduction products nitrosoarene and silyl formate are the key intermediates affording the most efficient C–N coupling for the *N,N*-dimethylation of nitroaromatics with CO<sub>2</sub>.

## Introduction

The emission of CO<sub>2</sub> due to the utilization of fossil energy accounts for the primary environmental issue of the greenhouse effect and global warming nowadays.<sup>1</sup> To alleviate such an issue and further achieve carbon neutrality, a variety of strategies using CO<sub>2</sub> as the sustainable C<sub>1</sub> surrogate in chemical synthesis have been documented. Therein, the reductive coupling of CO<sub>2</sub> and N-based nucleophiles leading to formamide, aminal, and methylamine through adjusting the selective 2e<sup>−</sup>, 4e<sup>−</sup>, and 6e<sup>−</sup> reduction of CO<sub>2</sub> attracts the most attention.<sup>2</sup> In this domain, a wide range of homogeneous catalysts<sup>3</sup> and heterogeneous catalysts,<sup>4</sup> coupled with the respective hydrogen source (H source), have been documented (Scheme 1A). Particularly, the *N*-formylation of amines with CO<sub>2</sub> and hydrosilanes even proceeded without catalysts,<sup>5</sup> which was promoted by the specific solvent dimethyl sulfoxide. By contrast, nitroaromatics, known as the readily available and cheap aniline precursors, are relatively underutilized in

the reductive C–N coupling reactions with CO<sub>2</sub> (Scheme 1B). The pioneering studies by Shi's group<sup>6</sup> and Liu's group<sup>7</sup> independently demonstrated that such a transformation is feasible by using Cu-based (CuAlO<sub>x</sub>) and Au-based (Au/TiO<sub>2</sub>) heterogeneous catalysts of different substrate tolerance. Mechanistic analysis suggested that it proceeds with the initial hydrogenation of nitroarene to aniline, followed by *N*-methylation with

A) The *N*-formylation of amines with CO<sub>2</sub>B) The *N*-methylation of nitroaromatics with CO<sub>2</sub>C) This work: Co-catalyzed *N,N*-dimethylation of nitroaromatics with CO<sub>2</sub>

**Scheme 1** Transition metal-mediated reductive C–N coupling with CO<sub>2</sub>.

<sup>a</sup>Beijing Key Laboratory of Ionic Liquids Clean Process, Key Laboratory of Green Process and Engineering, State Key Laboratory of Multiphase Complex Systems, Institution of Process Engineering, Chinese Academy of Sciences, Beijing 100190, China. E-mail: csl@ipe.ac.cn

<sup>b</sup>College of Chemistry and Chemical Engineering, University of Chinese Academy of Sciences, Beijing, 100049, China

<sup>c</sup>School of Chemistry and Chemical Engineering, Beijing Institute of Technology, Beijing 100081, China. E-mail: bhxu@bit.edu.cn

<sup>d</sup>College of Materials Science and Engineering, Huaqiao University, Xiamen 361021, China

†Electronic supplementary information (ESI) available. CCDC 2149710. For ESI and crystallographic data in CIF or other electronic format see DOI: <https://doi.org/10.1039/d3gc02517a>

‡These authors contributed to this article equally.

CO<sub>2</sub> via the formamide intermediate. Recently, Ma's group<sup>8</sup> described a straightforward *N*-formylation of nitroarenes with CO<sub>2</sub> and hydrosilane but in the presence of excess Fe powder. Impressively, they preliminarily supposed that both the amide ion ArNH<sup>−</sup> and the amide dianion ArN<sup>2−</sup> (rather than aniline) originated from the reduction of nitroarenes with Fe powder functioning as the reactive species to activate and couple with CO<sub>2</sub>.

To the best of our knowledge, no homogeneous catalysts for the reductive coupling of nitroaromatics with CO<sub>2</sub> are currently known. This aspect, coupled with our recent interest in non-noble Co-catalyzed hydrogenation and reductive coupling reactions, encouraged us to explore the potential cobalt complexes enabling the direct *N*-methylation/formylation of nitroaromatics with CO<sub>2</sub>. In fact, a few novel cobalt catalysts or catalytic systems for homogeneous hydrogenation of CO<sub>2</sub> have been disclosed with the implementation of a tailored ligand structure, including a combination of appropriate cobalt salts with multidentate phosphines (tetraphos/triphos/dmpe),<sup>9</sup> pincer-based cobalt complexes,<sup>10</sup> and half-sandwich pentamethylcyclopentadienyl cobaltic complexes (Cp\*Co<sup>III</sup>) with proton-responsive ligands.<sup>11</sup> Remarkably, the former two systems also witnessed further functionalization through *in situ* generating intermediates that can be trapped by adding nucleophiles (e.g., alcohols<sup>9d</sup> or amines<sup>10a</sup>), which delivered the corresponding ethers or amides. Meanwhile, literature surveys demonstrating cobalt complexes that enable the selective reduction of nitroarenes to arylamines are rather few. Several catalytically active systems bearing phthalocyanine Co<sup>II</sup> complexes,<sup>12</sup> trinuclear mixed valent Co<sup>II</sup>/Co<sup>III</sup>/Co<sup>II</sup> complexes,<sup>13</sup> pyrrole carboxamide chelated Co<sup>II</sup> complexes,<sup>14</sup> or tris(*N*-heterocyclic thioamide) Co<sup>III</sup> complexes<sup>15</sup> have been reported to date. Experimental investigations into the possible levels of cobalt-catalyzed hydrogenation of CO<sub>2</sub> and studies on the difference from that of nitroaromatics, with the same catalytic system, would advance the potential strategies of reductive coupling of both reactants.

Following this perspective, Leitner and co-workers demonstrated Co(<sup>NMe</sup>PNP)Cl<sub>2</sub>-catalyzed adaptive and selective hydrogenation of CO<sub>2</sub> with hydrosilanes individually to formic acid, formaldehyde, or methanol.<sup>16</sup> We thereby envisioned that the fabrication of Cp\*Co<sup>III</sup> complexes with proton/silane-responsive ligands may enable the catalytic reduction of unsaturated CO<sub>2</sub> and nitroarenes using hydrosilanes as the H source and the catalytic level could be modulated by a specific structure and composition. To this end, the phosphinesulfonate ligand was considered due to the tunable coordination modes of the sulfonate moiety therein, which has exhibited unique behaviors by cooperating with the chelated transition metals (e.g., Ru, Ir) in the hydro-functionalization.<sup>17</sup> However, the analogous cobalt complexes have not been accessed and the catalytic performance has been unexplored yet. In this study, the phosphinesulfonate Cp\*Co<sup>III</sup> complex (Co(dppbsa)) was prepared for the first time, which surprisingly enables the *N,N*-dimethylation of nitroaromatics with CO<sub>2</sub> and hydrosilanes (Scheme 1C).

## Results and Discussion

The half-sandwich phosphinesulfonate cobaltic complex (Co(dppbsa)) was accessed by neutralization of 2-(diphenylphosphanyl)benzenesulfonic acid with *t*BuOK, followed by a metathesis reaction with the metal precursor Cp\*Co(CO)I<sub>2</sub> (Cp\* = pentamethylcyclopentadiene anion). It features a typical methyl <sup>1</sup>H NMR (CDCl<sub>3</sub>, 298 K) peak at 1.41 ppm, corresponding to the presence of the Cp\* moiety. Besides, the phosphine <sup>31</sup>P{<sup>1</sup>H} NMR (243 MHz) peak down-field shifts from 3.8 ppm assigned for 2-(diphenylphosphanyl)benzenesulfonic acid to 33.4 ppm due to the coordination with the Co<sup>III</sup> center. The molecular structure of Co(dppbsa) was unambiguously determined by X-ray crystal diffraction analysis. In the solid state (Fig. 1 and Fig. S1†), the cobaltic center is surrounded by one iodo ligand, one pentamethylcyclopentadiene ligand, and one bidentate dppbsa ligand in a pseudo-octahedron geometry, which is reasonable for a d<sup>6</sup>(cobalt) high-spin configuration.

The benchmark reaction of nitrobenzene (**1a**) with CO<sub>2</sub> catalyzed by Co(dppbsa) was examined in the presence of stoichiometric hydrosilane as the H source (Table 1). To our delight, *N,N*-dimethylaniline (**2a**) was obtained with a high yield of 85% when the reaction of **1a** (0.2 mmol) with CO<sub>2</sub> (3 MPa) was conducted in the presence of Co(dppbsa) (5 mol%), NaBAR<sup>F</sup><sub>4</sub> (5 mol%), and a combination of PhSiH<sub>3</sub> (6 equiv.) and Et<sub>3</sub>SiH (15 equiv.) at 150 °C in toluene for 24 h under argon (entry 1). Such a *N,N*-dimethylation of **1a** with CO<sub>2</sub> did not proceed well without NaBAR<sup>F</sup><sub>4</sub> (entry 2), largely terminating at the amine (**3a**) and *N*-monomethylation (**4a**). By contrast, the reaction did not occur at all without Co(dppbsa) (entry 3). Both the activity and selectivity toward *N,N*-dimethylation decreased by lowering the reaction temperature to 130 °C (entry 4), but without delivering the *N*-formylation products. It has not benefited in improving the selectivity toward **2a** by increasing the initial pressure of CO<sub>2</sub> to 5 MPa, which instead promoted the

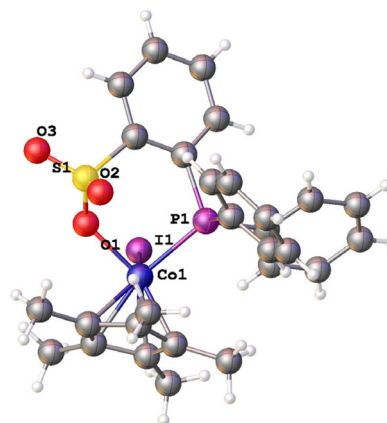


**Fig. 1** A view of the molecular structure of Co(dppbsa); Selected bond lengths [Å] and angles [°]: Co(1)–I(1) 2.5993(8), Co(1)–O(1) 1.965(5), Co(1)–P(1) 2.270(2); S(1)–O(1) 1.486(4), S(1)–O(2) 1.440(4), S(1)–O(3) 1.448(6); O(1)–Co(1)–P(1) 94.1(1).

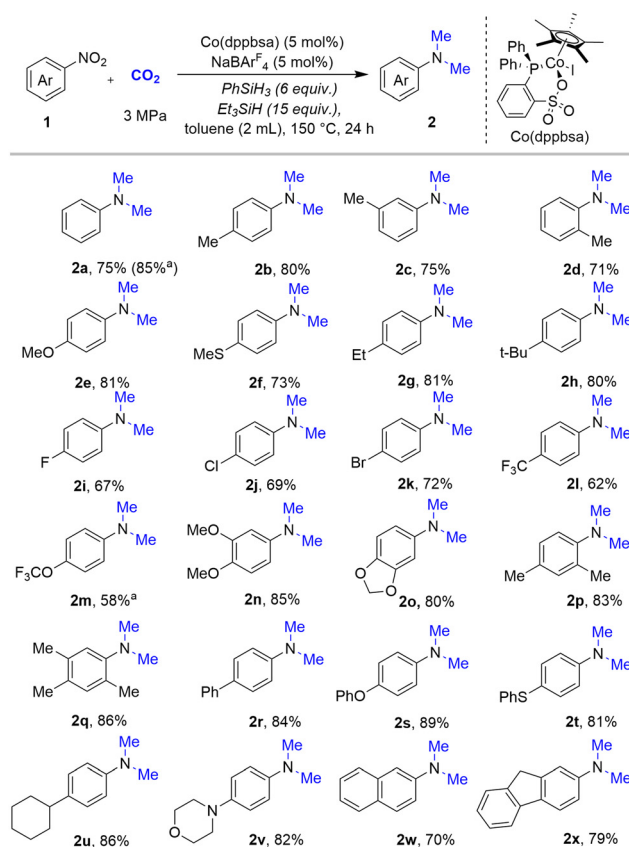
**Table 1** Screening the reaction conditions for *N,N*-dimethylation of **1a** with CO<sub>2</sub><sup>a</sup>

| <b>1a</b> + CO <sub>2</sub> $\xrightarrow[\text{toluene (2 mL), 130~150 } ^\circ\text{C}]{[\text{Co}] (0\sim5 \text{ mol\%}), \text{NaBARF}_4 (0\sim5 \text{ mol\%}), \text{hydrosilane}}$ <b>2a/3a/4a</b> |             |                            |                        |                               |
|--|-------------|----------------------------|------------------------|-------------------------------|
| <b>2a</b> (R <sup>1</sup> = R <sup>2</sup> = Me); <b>3a</b> (R <sup>1</sup> = R <sup>2</sup> = H); <b>4a</b> (R <sup>1</sup> = H, R <sup>2</sup> = Me)   |             |                            |                        |                               |
| Entry <sup>a</sup>   | [Co] (mol%) | NaBARF <sub>4</sub> (mol%) | Conv. <sup>b</sup> (%) | Yield <sup>b</sup> (%)        |
|  |             |                            |                        | <b>2a</b> <b>3a</b> <b>4a</b> |
| 1  | 5           | 5                          | 100                    | 85   4   0                    |
| 2  | 5           | 0                          | 100                    | 34   18   12                  |
| 3  | 0           | 5                          | 0                      | 0   0   0                     |
| 4 <sup>c</sup>   | 5           | 5                          | 83                     | 50   20   8                   |
| 5 <sup>d</sup>   | 5           | 5                          | 100                    | 70   20   2                   |
| 6 <sup>e</sup>   | 5           | 5                          | 65                     | 28   20   10                  |
| 7 <sup>f</sup>   | 5           | 5                          | 100                    | 41   20   3                   |
| 8 <sup>g</sup>   | 5           | 5                          | 37                     | 24   8   2                    |

<sup>a</sup> Reaction condition: **1a** (0.2 mmol, 1 equiv.), CO<sub>2</sub> (3.0 MPa), Co(dppbsa) (0–5 mol%), NaBARF<sub>4</sub> (0–5 mol%), hydrosilane (PhSiH<sub>3</sub> (6 equiv.), Et<sub>3</sub>SiH (15 equiv.)), toluene (2 mL), at 150 °C for 24 h, under argon. <sup>b</sup> Determined by GC analysis using biphenyl as the internal standard. <sup>c</sup> 130 °C. <sup>d</sup> CO<sub>2</sub> (5 MPa). <sup>e</sup> Cp\*Co(CO)I<sub>2</sub>. <sup>f</sup> PhSiH<sub>3</sub> (11 equiv.). <sup>g</sup> Et<sub>3</sub>SiH (33 equiv.).

reduction of **1a** to **3a**. Finally, the dppbsa ligand in Co(dppbsa) was found to be indispensable to achieve a high catalytic efficiency since the performance of its precursor (Cp\*Co(CO)I<sub>2</sub>) was much poor (entry 6). We also noticed that neither PhSiH<sub>3</sub> nor Et<sub>3</sub>SiH in a theoretically comparable amount with hydride could promote the desired C–N coupling independently (entries 7 and 8). Particularly, the presence of Et<sub>3</sub>SiH alone largely disables the reductive conversion of **1a** (entry 8). Further efforts on optimizing the reactivity by screening different hydrosilanes and solvents failed (Table S1†).

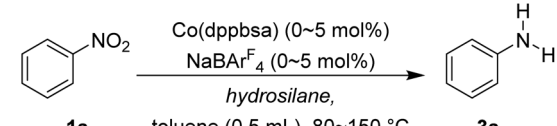
The scope and limitation of nitroaromatic substrates under the newly developed protocol were subsequently investigated (Scheme 2). Evidently, the electronic variation of substituents at the nitroaromatics affects the reaction efficiency. For instance, *N,N*-dimethyl arylamines substituted with electron-donating groups (EDGs), such as methyl (**2b**), methoxy (**2e**), methylthio (**2f**), ethyl (**2g**), tertiary butyl (**2h**), and cyclohexyl (**2u**), were obtained in higher yields as compared to those with electron-withdrawing groups (EWGs), such as fluoro (**2i**), chloro (**2j**), bromo (**2k**), trifluoromethyl (**2l**), and trifluoromethoxy (**2m**). The position of substituents at the nitroaromatics plays a minor role in the desired *N,N*-dimethylation process as demonstrated by the yield of *N,N*-dimethylanilines, which decreases in the order of *para*-(**2b**) > *meta*-(**2c**) > *ortho*-(**2d**). Remarkably, dehalogenation under such reduction conditions was not detected for **2i**–**2k**. Besides, the disubstituted, poly-substituted, and polycyclic aromatic nitroarenes proceeded satisfactorily, delivering **2p** (83%), **2q** (86%), **2r** (84%), **2s** (89%), **2w** (70%), and **2x** (79%) by reacting with CO<sub>2</sub>. Despite the steric hindrance, both the dimethyl-substituted **1p**

**Scheme 2** Co(dppbsa)-catalyzed *N,N*-dimethylation of nitroarenes with CO<sub>2</sub>. Reaction conditions: **1** (0.2 mmol), under argon, isolated yields. <sup>a</sup> Determined by GC analysis using biphenyl as the internal standard.

and the polymethyl-substituted **1q** are more reactive than the monomethyl-substituted **1b**–**1d** counterpart probably due to the electron-rich character. Heterocyclic nitroaromatics containing O, S, N atoms are also tolerated, providing **2o** (80%), **2s** (89%), **2t** (81%), and **2v** (82%) with excellent yields. The catalytic *N,N*-dimethylation of **1a** with CO<sub>2</sub> on a scale of 5 mmol was finally examined, which delivers **2a** in 75% isolated yield (Scheme S1†).

During the investigation of Co(dppbsa)-catalyzed *N,N*-dimethylation of nitrobenzene (**1a**) with CO<sub>2</sub>, the combination of Co(dppbsa) and NaBARF<sub>4</sub> was found to be capable of reducing **1a** to **3a** with hydrosilanes as the reductant. Further studies demonstrated that such a reduction proceeds moderately without feeding CO<sub>2</sub> (Table 2, entry 1). The presence of PhSiH<sub>3</sub> alone performed similarly (entry 2), largely terminating at the intermediates. In contrast, the reductive formation of **3a** was significantly promoted by changing PhSiH<sub>3</sub> to Et<sub>3</sub>SiH (entry 3). These results suggested that the coupling of Co(dppbsa) with PhSiH<sub>3</sub> is more reactive than that with Et<sub>3</sub>SiH in terms of the reduction of nitroaromatics, thereby inhibiting the activity of Et<sub>3</sub>SiH upon using a combination of PhSiH<sub>3</sub> and Et<sub>3</sub>SiH. We also observed that the activity of PhSiH<sub>3</sub> toward nitroaromatics has been basically maintained when feeding CO<sub>2</sub> (entry 4 vs.

**Table 2** Screening the reaction conditions for the catalytic reduction of **1a** to **3a**<sup>a</sup>

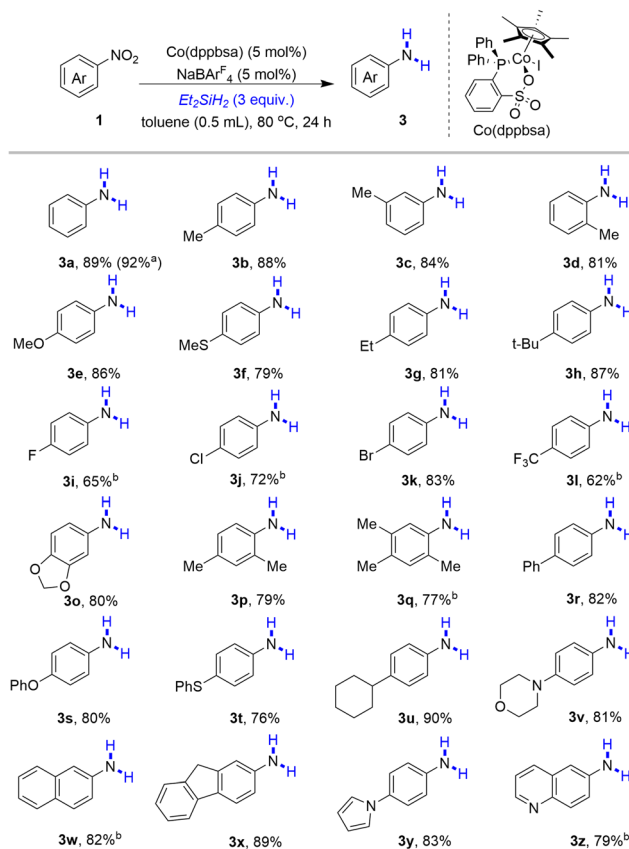
|  |   |                        |                        |
|---|---|------------------------|------------------------|
| Entry   | Variation from the "standard condition" <sup>a,b</sup>        | Conv. <sup>c</sup> (%) | Yield <sup>c</sup> (%) |
| 1   | PhSiH <sub>3</sub> (6.0) + Et <sub>3</sub> SiH (15.0), 150 °C | 100                    | 37                     |
| 2   | PhSiH <sub>3</sub> (6.0), 150 °C                              | 100                    | 30                     |
| 3   | Et <sub>3</sub> SiH (15.0), 150 °C                            | 100                    | 89                     |
| 4 <sup>d</sup>  | PhSiH <sub>3</sub> (6.0), CO <sub>2</sub> (3 MPa), 150 °C     | 100                    | 24                     |
| 5 <sup>e</sup>  | Et <sub>3</sub> SiH (15.0), CO <sub>2</sub> (3 MPa), 150 °C   | 30                     | 0                      |
| 6   | Et <sub>3</sub> SiH (15.0)                                    | 100                    | 87                     |
| 7   | Et <sub>3</sub> SiH (6.0)                                     | 100                    | 82                     |
| 8   | (EtO) <sub>3</sub> SiH (6.0)                                  | 100                    | 80                     |
| 9   | TMDSO (3.0)   | 100                    | 76                     |
| 10  | —   | 100                    | 92                     |
| 11  | No NaBARF <sub>4</sub>  | 30                     | 16                     |
| 12  | No Co(dppbsa)   | 10                     | 6                      |

<sup>a</sup> Standard condition: **1a** (0.2 mmol), Co(dppbsa) (5 mol%), NaBARF<sub>4</sub> (5 mol%), Et<sub>3</sub>SiH<sub>2</sub> (3 equiv.), toluene (2 mL), 80 °C, 24 h, under argon.

<sup>b</sup> Hydrosilane (x equiv.). <sup>c</sup> Determined by GC analysis using biphenyl as the internal standard. <sup>d</sup> Yield: **2a** (35%), **4a** (4%). <sup>e</sup> Yield: **2a** (24%), **4a** (4%).

entry 2), while the reduction of **1a** with Et<sub>3</sub>SiH was highly inhibited in the presence of CO<sub>2</sub> (entry 5 vs. entry 3). It signified the preferential reduction of CO<sub>2</sub> with Et<sub>3</sub>SiH rather than PhSiH<sub>3</sub> under the cobalt catalysis. In addition, it allows for reducing the reaction temperature (entry 6) and the dosage of Et<sub>3</sub>SiH (entry 7) without remarkably losing the reactivity of reduction with Et<sub>3</sub>SiH. The reaction efficiency was thereafter improved by screening different hydrosilanes (entries 8–10). As a result, the best yield of 92% was obtained when the reduction of **1a** (0.2 mmol) with diethylsilane (Et<sub>2</sub>SiH<sub>2</sub> (3 equiv.)) was conducted with Co(dppbsa) (5 mol%) and NaBARF<sub>4</sub> (5 mol%) in toluene at 80 °C for 24 h (entry 9). Noteworthily, the combination of Co(dppbsa) and NaBARF<sub>4</sub> was a prerequisite to reach such a high reactivity (entries 11 and 12).

The functional group tolerance of nitroaromatics in the reductive transformation to amines was also examined (Scheme 3). Notably, nitroaromatics substituted with EDGs, such as methyl (**1b**), methoxy (**1e**), methylthio (**1f**), ethyl (**1g**), tertiary butyl (**1h**), and cyclohexyl (**1u**), performed slightly poorer as compared to that without a substituent (**1a**). However, the introduction of EWGs, such as fluoro (**1i**), chloro (**1j**), bromo (**1k**), and trifluoromethyl (**1l**), did not show better results. Particularly, the reduction of **1i**, **1j** and **1l** needs to be conducted at a higher temperature of 120 °C to ensure satisfactory reactivity. This suggested that the rate-limiting step for the Co(dppbsa)-catalyzed reduction of nitroaromatics with Et<sub>2</sub>SiH<sub>2</sub> may vary with the different electronic effects of substrates. Again, the dehalogenation was not detected in the formation of **3i–3k**. The steric effect is also unfavorable for such a trans-



**Scheme 3** Co(dppbsa)-catalyzed reduction of nitroaromatics (**1**) with Et<sub>2</sub>SiH<sub>2</sub>. Reaction conditions: **1** (0.2 mmol), under argon, isolated yields (as the chloride salt counterparts). <sup>a</sup> Determined by GC analysis using biphenyl as the internal standard. <sup>b</sup> Reaction temperature: 120 °C.

formation, thereby delivering anilines in the decreasing order of *para*-(**3b**) > *meta*-(**3c**) > *ortho*-(**3d**). Herein, the dimethyl-substituted (**1p**) and polymethyl-substituted (**1p**) nitroaromatics perform poorer than the monomethyl-substituted **1b–1d** counterpart due to the electron-rich character combined with steric hindrance. At the same time, polycyclic nitroaromatics are well tolerated (**3r–3z**). Remarkably, nitroaromatics bearing medically relevant building blocks also survived with such a system, delivering anilines containing morpholine (**3v**), pyrrole (**3y**) and quinoline (**3z**) scaffolds with excellent chemo-selectivity.

To discern the required number of electron transfer in the reduction of CO<sub>2</sub> for C–N coupling, the catalytic hydrosilylation of CO<sub>2</sub> with hydrosilanes in C<sub>6</sub>D<sub>6</sub> was examined. Representatively, the distribution of silylated products after reacting for 4 hours was analyzed (Fig. 2) by quantitative <sup>13</sup>C {<sup>1</sup>H} NMR spectroscopy according to the previous reports,<sup>18</sup> wherein the silyl formate units, the bis(silyl)acetal units, and the methoxy-silane units could be finely identified. As a result, the combination of Co(dppbsa) and NaBARF<sub>4</sub> mainly promoted the two-electron reduction of CO<sub>2</sub> to give silyl formate (Fig. 2A), whereas the six-electron reduction leading to methoxysilane also moderately occurred. By contrast, the Co(dppbsa)-



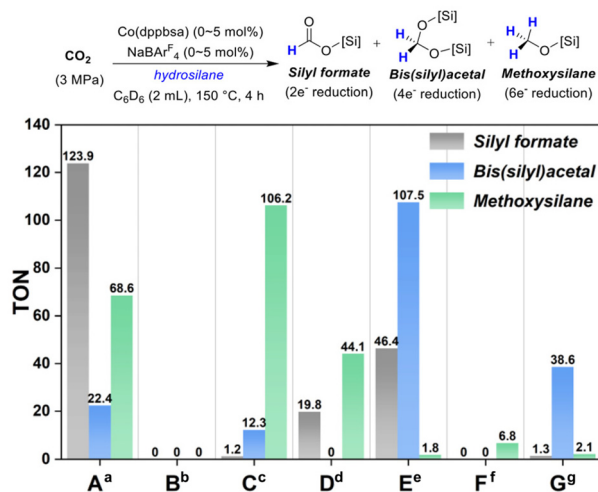


**Fig. 2** Catalytic hydrosilylation of CO<sub>2</sub>. Reaction conditions: hydrosilane (PhSiH<sub>3</sub> (6 equiv.) and Et<sub>3</sub>SiH (15 equiv.)), under argon. <sup>a</sup> Co(dppbsa) (5 mol%), NaBAR<sub>4</sub><sup>F</sup> (5 mol%). <sup>b</sup> Co(dppbsa) (5 mol%). <sup>c</sup> NaBAR<sub>4</sub><sup>F</sup> (5 mol%). <sup>d</sup> Co(dppbsa) (5 mol%), NaBAR<sub>4</sub><sup>F</sup> (5 mol%), PhSiH<sub>3</sub> (11 equiv.), without Et<sub>3</sub>SiH. <sup>e</sup> Co(dppbsa) (5 mol%), NaBAR<sub>4</sub><sup>F</sup> (5 mol%), Et<sub>3</sub>SiH (33 equiv.), without PhSiH<sub>3</sub>. <sup>f</sup> NaBAR<sub>4</sub><sup>F</sup> (5 mol%), PhSiH<sub>3</sub> (11 equiv.), without Et<sub>3</sub>SiH. <sup>g</sup> NaBAR<sub>4</sub><sup>F</sup> (5 mol%), Et<sub>3</sub>SiH (33 equiv.), without PhSiH<sub>3</sub>.

catalyzed hydrosilylation of CO<sub>2</sub> did not occur at all without NaBAR<sub>4</sub><sup>F</sup> (Fig. 2B), while the six-electron reduction was significantly preferred with NaBAR<sub>4</sub><sup>F</sup> alone (Fig. 2C). Furthermore, the activity of PhSiH<sub>3</sub> is obviously lower than that of Et<sub>3</sub>SiH in the catalytic hydrosilylation of CO<sub>2</sub> regardless of the presence (Fig. 2D vs. Fig. 2E) or the absence (Fig. 2F vs. Fig. 2G) of Co(dppbsa). It's consistent with the results of cross-experiments on the catalytic reduction of **1a** to **3a** (Table 2, entries 2–5). Meanwhile, these independent experiments signified the cooperative effect present not only between Co(dppbsa) and NaBAR<sub>4</sub><sup>F</sup> (Fig. 2A vs. Fig. 2B vs. Fig. 2C), but also between PhSiH<sub>3</sub> and Et<sub>3</sub>SiH (Fig. 2A vs. Fig. 2D vs. Fig. 2E or Fig. 2C vs. Fig. 2F vs. Fig. 2G) in the catalytic hydrosilylation of CO<sub>2</sub>, resulting in different reactivities and product distributions.

The performance of C1 surrogates derived from the hydrogenation of CO<sub>2</sub>, such as HCOOH, CO, (CH<sub>2</sub>O)<sub>n</sub>, and MeOH, was further examined in the Co(dppbsa)-catalyzed *N*-methylation of **1a** (Fig. 3). As a result, neither MeOH nor CO allowed for the C–N coupling, which instead moderately delivered the reduction product of **3a**. For the reactions with CO feedstock, a diluted CO by coincidentally feeding N<sub>2</sub> was introduced to prevent the potential deactivation of the cobalt catalyst. Evidently, the result was almost unchanged by modulating the partial pressure of CO. By contrast, the *N,N*-dimethylation of **1a** with either HCOOH or (CH<sub>2</sub>O)<sub>n</sub> occurs, despite providing only a moderate yield of **2a**. Combined with the catalytic performance of hydrosilylation of CO<sub>2</sub> under the standard conditions (Fig. 2A), we reasonably proposed that the silyl formate or its analogue acts as the carbon-based intermediate while participating in the C–N coupling step.

To approach the reductive C–N coupling, nitroarene (**1a**) might be parallelly transformed to nitrosoarene (**5a**), *N*-aryl

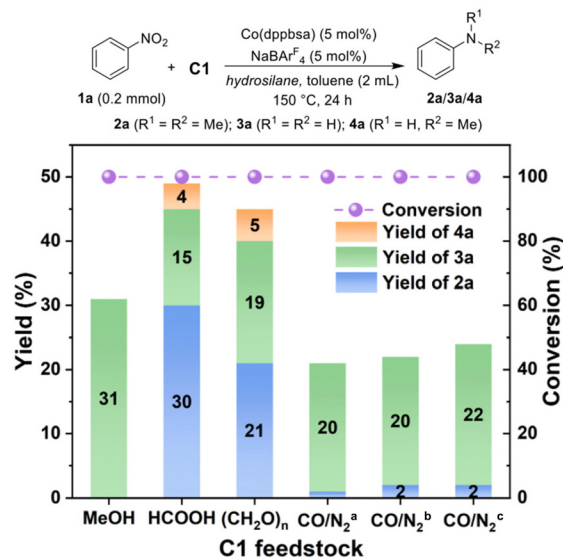


**Fig. 3** Reaction of possible C1 intermediates. Reaction conditions: hydrosilane (PhSiH<sub>3</sub> (6 equiv.) and Et<sub>3</sub>SiH (15 equiv.)), C1 feedstock (1.0 mmol), under argon. <sup>a</sup> CO/N<sub>2</sub> (1.0/2.0 MPa). <sup>b</sup> CO/N<sub>2</sub> (0.5/2.5 MPa). <sup>c</sup> CO/N<sub>2</sub> (0.1/2.9 MPa). <sup>d</sup> Yields were determined by GC analysis using biphenyl as the internal standard.

hydroxylamine (**5b**), azoxyarene (**5c**), azoarene (**5d**), and even aniline (**3a**).<sup>19</sup> The reactivity of these N-based substrates (N-Sub) with CO<sub>2</sub> was examined under the optimum conditions (Fig. 4a and b), respectively, to identify the most likely N-based intermediates in the catalytic cycle of *N*-methylation of nitroaromatics. Evidently, both **3a** and **5a** led to **2a** with an over 70% yield (Fig. 4b). By contrast, the *N*-methylation of the other nitrogen-based species (**5b–5d**), documented as the intermediates of the condensation route leading to **3a**,<sup>19</sup> performed worse. Furthermore, the time-course plots for the *N,N*-dimethylation of **1a**, **3a**, and **5a** within the first 8 hours were obtained and compared (Fig. 4c and Fig. S3†). They demonstrated that the rate leading to **2a** from **3a** is remarkably slower than that from the other two substrates. Besides, the mass-balance for **5a** contains a significant amount of **4a** (Fig. S3†), which distributed in a pyramid shape along the reaction time, suggesting that the *N*-methylation of **5a** with CO<sub>2</sub> by C–N coupling is too fast to form the hydrodeoxygenation product of **3a**. Thus, the possibility of amines as the major intermediate was excluded. Thereafter, it's confirmed by the competitive experiment using an equal amount of nitroaromatic (**1e**) and aniline (**3a**) as the N-Sub, which mainly provided **2e** via *N,N*-dimethylation of **1e** (Fig. 4d). As such, the nitrosoarene (**5a**) was the most reactive intermediate in the C–N coupling step.

Based on our results and the related processes, we proposed a tentative route for the Co(dppbsa)-catalyzed reductive *N,N*-dimethylation of nitroaromatics with CO<sub>2</sub> and hydrosilanes in Scheme 4A. In general, the reduction of nitroarene occurs along with that of CO<sub>2</sub>, using different hydrosilanes or their combination as the preferred H source. The structural variation of Co(dppbsa) during the catalysis cannot be specified at

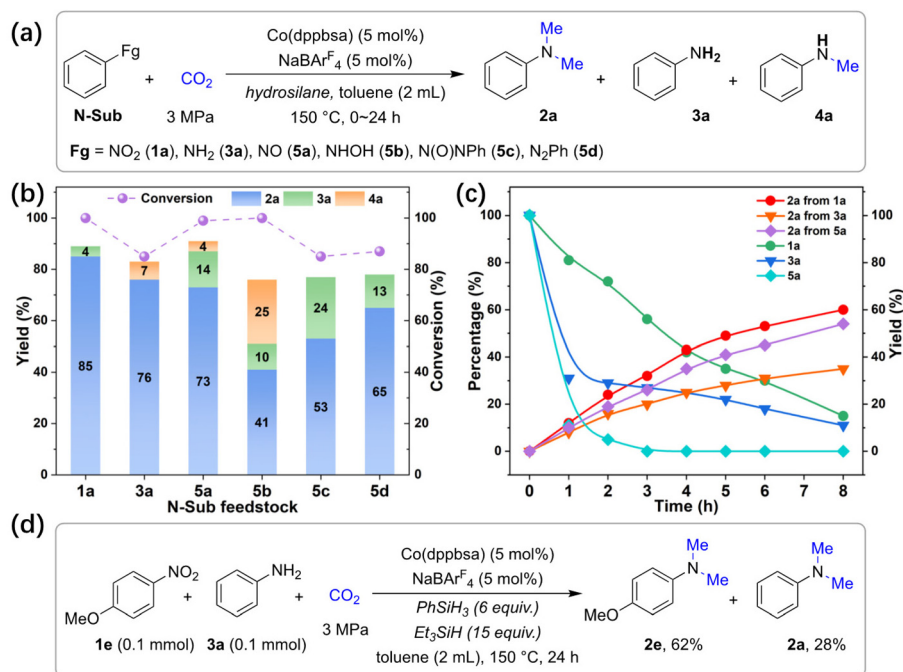
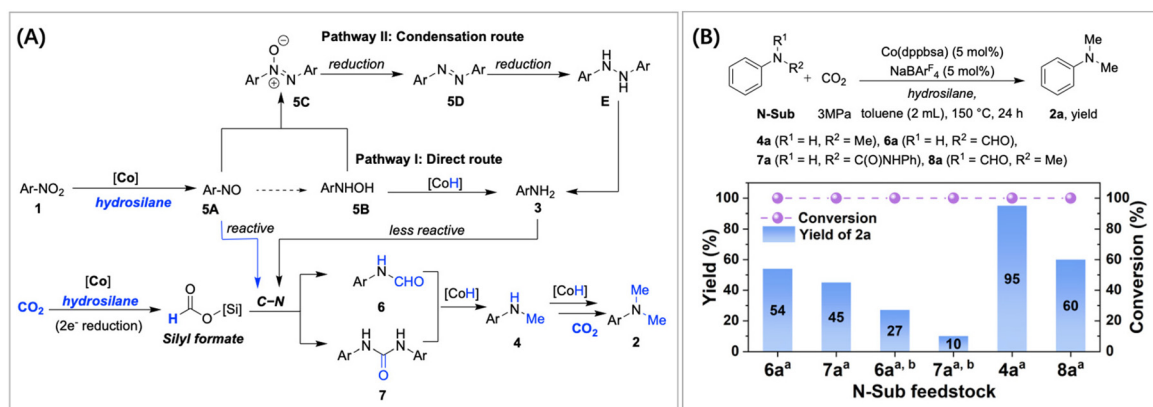


**Fig. 4** (a) Reaction of possible N-containing intermediates. Reaction conditions: hydrosilane (PhSiH<sub>3</sub> (6 equiv.) and Et<sub>3</sub>SiH (15 equiv.)), under argon. <sup>a</sup> Conversion and yield were determined by GC analysis using biphenyl as the internal standard. (b) Reaction of possible N-containing intermediates. (c) The time-course plots for the reaction of intermediates. (d) Competitive experiment of 4-nitroanisole (1e) with aniline (3a).

present. However, a considerable amount of Cp\* was detected by GC-MS analysis in the evaluation of the catalytic performance (Fig. S4†), suggesting that the cobalt center bears at least six coordination vacancies during the catalysis as Ru(dppbsa).<sup>19</sup> Both nitrosoarene (5A) and silyl formate were recognized as the key intermediates participating in the desired C–N coupling, leading to either N-formylation 6<sup>6</sup> or diaryl urea 7.<sup>20</sup> It thus exhibits an apparent cooperative effect between two hydrosilanes (PhSiH<sub>3</sub> and Et<sub>3</sub>SiH) since the formation rates of nitrosoarene (5A) and silyl formate are modulated by both the structures and proportions. Despite the ambiguity of multi-step reduction, it's strongly suggested by

the experimental results that the silane involved in the catalysis follows an outer-sphere ionic hydrosilylation mechanism.<sup>21</sup> The schematic illustration of Co(dppbsa)-catalyzed reduction of unsaturated bonds with silane was preliminarily supposed as given in Scheme S2,† taking the reduction of CO<sub>2</sub> to silyl formate as an example. Despite being less reactive, the reductive coupling with anilines (3) cannot be completely excluded from the overall catalytic process due to the readily reduction of 5A either by the direct route *via* hydroxylamine intermediates (5B) (Pathway I) or by the condensation route (Pathway II) *via* intermediates 5C, 5D, and E.<sup>22</sup> Next, the role of the N-formylation product and diaryl urea as the potential inter-



**Scheme 4** (A) Proposed reaction pathway in the Co(dppbsa)-catalyzed reductive N,N-dimethylation of nitroaromatics with CO<sub>2</sub> and hydrosilanes. (B) General conditions: N-Sub (0.2 mmol). <sup>a</sup> PhSiH<sub>3</sub> (6 equiv.), Et<sub>3</sub>SiH (15 equiv.). <sup>b</sup> No Co(dppbsa).

mediate in the reductive *N,N*-dimethylation of nitroaromatics with CO<sub>2</sub> was examined (Scheme 4B). The performances of **6a** and **7a** under the standard conditions are comparable (yield of **2a**: **6a**, 54%; **7a**, 45%), indicating that both are possible. However, the yield of **2a** obtained from these N-based intermediates containing the carbonyl moiety is apparently lower than that from the nitroaromatic precursor (**1a**, 92%). It could be attributed to the deregulated reduction rate of N-Sub (**6a**/**7a**) and CO<sub>2</sub>, thereby negatively affecting the efficiency of consequent C–N coupling. Evidently, NaBAR<sup>F</sup><sub>4</sub> alone, which was previously proved to be active for the catalytic hydrosilylation of CO<sub>2</sub> (Fig. 2C), also enables the full conversion of **6a** and **7a** but with much worse yields of **2a** (27% and 10%). Efforts on isolating and identifying the species for the mass imbalance by basic hydrolysis and GC-MS analysis failed (Fig. S5†), suggesting that high boiling point products had been generated. We therefore supposed that these labile carbonyl groups at the intermediates towards the hydrosilanes account for the unidentified species during the independent examinations by launching a large dosage. It's further confirmed by the comparison between **4a** (without the carbonyl group) and **8a** (with the carbonyl group), which delivers **2a** with yields of 95% and 60%, respectively, under the standard conditions.

## Conclusion

In summary, the preparation method and the catalytic performance of a half-sandwich phosphinesulfonate cobaltic complex (Co(dppbsa)) were studied. Remarkably, the combination of Co(dppbsa) and NaBAR<sup>F</sup><sub>4</sub> enables the chemoselective catalytic reduction of not only nitroaromatics, but also CO<sub>2</sub> by taking appropriate hydrosilanes as the reductant. It thus allows for the reductive coupling of nitroaromatics with CO<sub>2</sub> by modulating the catalytic level with a specific structure and composition of hydrosilanes. As a result, the Co(dppbsa)-catalyzed reductive *N,N*-dimethylation of nitroaromatics with CO<sub>2</sub> was approached with a combination of PhSiH<sub>3</sub> and Et<sub>3</sub>SiH of a specific proportion. Mechanistic experiments suggested that the semi-reduction products nitrosoarene and silyl formate are the key intermediates participating in the desired C–N coupling. This study provides an efficient protocol for the high-value utilization of CO<sub>2</sub> catalyzed by non-noble cobalt. The versatile reactivity of phosphinesulfonate chelated transition metal complexes in reductive coupling deserves further exploration.

## Author contributions

Shuang-Shuang Ma: investigation, data curation, and formal analysis. Rui Sun: data curation, formal analysis, and validation. Zi-Heng Zhang: formal analysis, visualization and writing – review and editing. Peng-Xin Guan: data curation. Jin-Qing Lin: writing – review. Chun-Shan Li: supervision. Bao-

Hua Xu: conceptualization, methodology, writing – original draft, supervision, and project administration.

## Conflicts of interest

There are no conflicts to declare.

## Acknowledgements

Financial support from the Excellent Young Scientists Fund (22022815) and the National Natural Science Foundation of China (22178346) is gratefully acknowledged.

## References

- (a) J. Artz, T. E. Muller, K. Thenert, J. Kleinekorte, R. Meys, A. Sternberg, A. Bardow and W. Leitner, *Chem. Rev.*, 2018, **118**, 434–504; (b) C. Figueres, C. Le Quéré, A. Mahindra, O. Bäte, G. Whiteman, G. Peters and D. Guan, *Nature*, 2018, **564**, 27–30; (c) D. Shindell and C. J. Smith, *Nature*, 2019, **573**, 408–411.
- (a) X. F. Liu, X. Y. Li, C. Qiao, H. C. Fu and L. N. He, *Angew. Chem., Int. Ed.*, 2017, **56**, 7425–7429; (b) C. Xie, J. Song, H. Wu, B. Zhou, C. Wu and B. Han, *ACS Sustainable Chem. Eng.*, 2017, **5**, 7086–7092; (c) Z.-J. Mu, X. Ding, Z.-Y. Chen and B.-H. Han, *ACS Appl. Mater. Interfaces*, 2018, **10**, 41350–41358.
- (a) U. Jayarathne, N. Hazari and W. H. Bernskoetter, *ACS Catal.*, 2018, **8**, 1338–1345; (b) X.-D. Li, S.-M. Xia, K.-H. Chen, X.-F. Liu, H.-R. Li and L.-N. He, *Green Chem.*, 2018, **20**, 4853–4858; (c) Z. Huang, X. Jiang, S. Zhou, P. Yang, C. X. Du and Y. Li, *ChemSusChem*, 2019, **12**, 3054–3059; (d) H. Liu, Z. Nie, J. Shao, W. Chen and Y. Yu, *Green Chem.*, 2019, **21**, 3552–3555; (e) Q. Zhang, X.-T. Lin, N. Fukaya, T. Fujitani, K. Sato and J.-C. Choi, *Green Chem.*, 2020, **22**, 8414–8422; (f) Z. Ke, Y. Zhao, R. Li, H. Wang, W. Zeng, M. Tang, B. Han and Z. Liu, *Green Chem.*, 2021, **23**, 9147–9153.
- (a) X. Cui, Y. Zhang, Y. Deng and F. Shi, *Chem. Commun.*, 2014, **50**, 13521–13524; (b) W. Lin, H. Cheng, Q. Wu, C. Zhang, M. Arai and F. Zhao, *ACS Catal.*, 2020, **10**, 3285–3296; (c) Y. Shen, Q. Zheng, Z. N. Chen, D. Wen, J. H. Clark, X. Xu and T. Tu, *Angew. Chem., Int. Ed.*, 2021, **60**, 4125–4132; (d) Z.-Z. Yang, B. Yu, H. Zhang, Y. Zhao, G. Ji and Z. Liu, *RSC Adv.*, 2015, **5**, 19613–19619.
- H. Lv, Q. Xing, C. Yue, Z. Lei and F. Li, *Chem. Commun.*, 2016, **52**, 6545–6548.
- X. Cui, X. Dai, Y. Zhang, Y. Deng and F. Shi, *Chem. Sci.*, 2014, **5**, 649–655.
- L. Hao, Y. Zhao, B. Yu, H. Zhang, H. Xu and Z. Liu, *Green Chem.*, 2014, **16**, 3039–3044.
- N. Shen, S.-J. Zhai, C. W. Cheung and J.-A. Ma, *Chem. Commun.*, 2020, **56**, 9620–9623.

- 9 (a) H. Gao, L. Chen, J. Chen, Y. Guo and D. Ye, *Catal. Sci. Technol.*, 2015, **5**, 1006–1013; (b) S. A. Burgess, A. M. Appel, J. C. Linehan and E. S. Wiedner, *Angew. Chem., Int. Ed.*, 2017, **56**, 15002–15005; (c) M. S. Jeletic, E. B. Hulley, M. L. Helm, M. T. Mock, A. M. Appel, E. S. Wiedner and J. C. Linehan, *ACS Catal.*, 2017, **7**, 6008–6017; (d) B. G. Schieweck and J. Klankermayer, *Angew. Chem., Int. Ed.*, 2017, **56**, 10854–10857; (e) J. Schneidewind, R. Adam, W. Baumann, R. Jackstell and M. Beller, *Angew. Chem., Int. Ed.*, 2017, **56**, 1890–1893.
- 10 (a) P. Daw, S. Chakraborty, G. Leitus, Y. Diskin-Posner, Y. Ben-David and D. Milstein, *ACS Catal.*, 2017, **7**, 2500–2504; (b) M. R. Mills, C. L. Barnes and W. H. Bernskoetter, *Inorg. Chem.*, 2018, **57**, 1590–1597.
- 11 Y. M. Badiei, W. H. Wang, J. F. Hull, D. J. Szalda, J. T. Muckerman, Y. Himeda and E. Fujita, *Inorg. Chem.*, 2013, **52**, 12576–12586.
- 12 W. Li, J. Artz, C. Broicher, K. Junge, H. Hartmann, A. Besmehn, R. Palkovits and M. Beller, *Catal. Sci. Technol.*, 2019, **9**, 157–162.
- 13 S. Srivastava, M. S. Dagur, A. Ali and R. Gupta, *Dalton Trans.*, 2015, **44**, 17453–17461.
- 14 S. Yadav, S. Kumar and R. Gupta, *Inorg. Chem. Front.*, 2017, **4**, 324–335.
- 15 D. I. Ioannou, D. K. Gioftsidou, V. E. Tsina, M. G. Kallitsakis, A. G. Hatzidimitriou, M. A. Terzidis, P. A. Angaridis and I. N. Lykakis, *J. Org. Chem.*, 2021, **86**, 2895–2906.
- 16 H. H. Cramer, B. Chatterjee, T. Weyhermuller, C. Werle and W. Leitner, *Angew. Chem., Int. Ed.*, 2020, **59**, 15674–15681.
- 17 (a) F. Jiang, K. Yuan, M. Achard and C. Bruneau, *Chemistry*, 2013, **19**, 10343–10352; (b) A. Labed, F. Jiang, I. Labed, A. Lator, M. Peters, M. Achard, A. Kabouche, Z. Kabouche, G. V. M. Sharma and C. Bruneau, *ChemCatChem*, 2015, **7**, 1090–1096.
- 18 H. H. Cramer, S. Ye, F. Neese, C. Werle and W. Leitner, *JACS Au*, 2021, **1**, 2058–2069.
- 19 (a) S.-S. Ma, R. Sun, Z.-H. Zhang, Z.-K. Yu and B.-H. Xu, *Org. Chem. Front.*, 2021, **8**, 6710–6719; (b) R. Sun, S. S. Ma, Z. H. Zhang, Y. Q. Zhang and B. H. Xu, *Org. Biomol. Chem.*, 2023, **21**, 1450–1456.
- 20 Y. Li, X. Fang, K. Junge and M. Beller, *Angew. Chem., Int. Ed.*, 2013, **52**, 9568–9571.
- 21 (a) M. Iglesias, F. J. Fernández-Alvarez and L. A. Oro, *ChemCatChem*, 2014, **6**, 2486–2489; (b) J. Yang, P. S. White and M. Brookhart, *J. Am. Chem. Soc.*, 2008, **130**, 17509–17518.
- 22 H. U. Blaser, *Science*, 2006, **313**, 312–313.